Macromolecules **2004,** *37,* 8342−8348

Preparation of a Zero-Birefringence Polymer Doped with a Birefringent Crystal and Analysis of Its Characteristics

Hisanori Ohkita,* Akihiro Tagaya, and Yasuhiro Koike

Faculty of Science and Technology, Keio University, 3-14-1 Hiyoshi, Kouhoku-ku, Yokohama 223-0061, Japan, and ERATO Koike Photonics Polymer Project, Japan Science and Technology Agency, E-building, K^2 Town Campus, 144-8 Ogura, Saiwai-ku, Kawasaki 212-0054, Japan

Received April 10, 2004; Revised Manuscript Received August 2, 2004

ABSTRACT: We proposed the "birefringent crystal dopant method" in order to compensate the birefringence of polymers. In this method, the birefringence was compensated by homogeneous doping with a needlelike crystal which has the opposite birefringence to that of the polymers. Strontium carbonate ($SrCO_3$) was selected for this purpose because it has a large birefringence and a needlelike shape. $SrCO_3$ was synthesized, with a length of about 200 nm and a width of about 20 nm, and doped into a poly(MMA/BzMA=78/22(w/w)) film. The film was drawn at 130 °C and 4 mm/min. The orientational birefringence of the drawn polymer film at a wavelength of 633 nm was compensated by doping with 0.3 wt % $SrCO_3$ without losing its transparency and thermostability. The analysis of infrared dichroism of the films showed that the birefringence of the films was compensated at a low concentration of $SrCO_3$ because of its orientation-inhibition effect and its high orientation degree as compared with that of the polymer main chains.

I. Introduction

Optical devices that can transmit, display, and store mass information are indispensable to the modern information-oriented society. Many optical devices based on polymer materials have attracted attention for use in recent optical technology, for example, polymer optical fibers,[1,2] functional films for liquid-crystal displays,[3] optical disks,[4] lenses,[5] and optical waveguides.[6] Polymers for precision optical devices have the advantage of easy processing, easy handling, light weight, and low cost as compared with glasses. However, the uses of polymers have one serious drawback: they are birefringent.

Birefringence comes from the anisotropic structure of a material. It was discovered as the double refraction phenomenon in calcite by Bartholinus in 1669.[7] If a narrow beam of natural light is sent into a birefringent material, it will split and emerge as two parallel beams with two refractive indices n_e and n_o, where n_e is a refractive index for the extraordinary rays and n_o is a refractive index for the ordinary rays. The refractive index n_e changes with the incident direction of light. Generally, birefringence Δn is defined by

$$\Delta n = n_e - n_o \qquad (1)$$

Many types of birefringence are widely studied in the field of optics, for example birefringence of a crystal,[7,8] intrinsic birefringence,[9] form birefringence,[8,10] and flow birefringence.[11,12] Birefringence of a crystal is caused by an anisotropy in the binding force on the electrons of atoms which compose the crystal. Intrinsic birefringence results from the polarizability anisotropy of polymer molecules. Form birefringence is caused by the ordered arrangement of similar particles of optically isotropic material whose size is large compared with the dimensions of molecules but small compared with the wavelength of light. Flow birefringence is known as the birefringence that is caused by the flow of polymer melts and solutions.

Birefringence degrades the performance of optical devices that require focusing by lenses or maintaining the polarization state of incident light. Birefringence does not occur if the polymer structure is perfectly random. Birefringence is caused by polymer chain orientation during a melt flowing and cooling stage in injection molding, extrusion, or drawing processing. This birefringence of a polymer is called orientational birefringence. In the case of uniaxially drawn polymer samples, orientational birefringence Δn is defined as

$$\Delta n = n_{\parallel} - n_{\perp} \qquad (2)$$

where $n_{\parallel}$ and $n_{\perp}$ are refractive indices for incident light polarized parallel and perpendicular to the draw direction, respectively. Positive polymers show orientational birefringence $\Delta n > 0$, and negative polymers show $\Delta n < 0$.

The polymer blend method[9,13] is a well-known compensation method for preparing zero-birefringence polymers that exhibit no birefringence for any orientation degree of polymer chains. In the method, positive and negative orientational birefringent homopolymers are blended. However, this procedure requires compatibility between both polymers. In addition, a blending partner is needed with a much higher birefringence value and opposite sign compared to those of the base polymer to compensate birefringence sufficiently. It is difficult to find such a polymer. To prepare zero-birefringence polymers, we proposed two methods: the random copolymerization method[14,15] and the anisotropic molecule dopant method.[16,17] Two types of monomers that produce positive and negative birefringent polymers were randomly copolymerized. A rodlike molecule that has a polarizability anisotropy was chosen and doped into polymers by the anisotropic molecule dopant method. The negative birefringence of poly(methyl methacrylate)

---

* Corresponding author: Ph +81-44-580-1563, Fax +81-44-580-1433, e-mail hisanori@2000.jukuin.keio.ac.jp.

10.1021/ma049296+ CCC: $27.50

(PMMA)-based polymers was compensated by both the methods.

The purpose of this article is to demonstrate the compensation of the birefringence of a polymer by the "birefringent crystal dopant method"[18] and to analyze the characteristics of the zero-birefringence polymer obtained. This article is organized as follows: We explain the compensation mechanism of this method in section II. In section III, we present experimental details to prepare and analyze the zero-birefringence polymer. Experimental results are described, and the optical and thermal characterizations of the polymer obtained are discussed in section IV. Finally, a summary of this study is presented in section V.

II. Birefringent Crystal Dopant Method

In the birefringent crystal dopant method, an inorganic birefringent crystal is homogeneously doped in a polymer and compensates the birefringence of the polymer. The crystal used for this method must have a needlelike or a rodlike shape and the opposite orientational birefringence to that of the polymer. The sign of the orientational birefringence of the crystal is defined in the same way as that of the polymers in this article. A crystal in a polymer is oriented to the direction of its long axis by tensile stress. Therefore, a positive orientational birefringent crystal has a higher refractive index in the direction of its long axis, and a negative crystal has a higher refractive index in its short axis direction. Furthermore, the crystal must be less than the size of an optical wavelength in order to form an optically isotropic medium. If the size of the crystal is too much larger than a wavelength to form an optically isotropic medium, the light transmitted through the crystal and the light transmitted through the polymer around the crystal become independent of each other. The mechanism of the compensation of orientational birefringence by the birefringent crystal dopant method is shown in Figure 1. Ellipsoids represent polarizability anisotropies of a monomer unit and a crystal, respectively. In the completely random state, polymer chains and crystals exhibit no birefringence as shown in Figure 1a. When the polymer chains are oriented during polymer processing as shown in Figure 1b, the crystals are also oriented because of their shape, and the birefringence of the crystals compensate the birefringence of the polymer. The orientational birefringence of positive and negative polymers can be compensated by a small amount of negative and positive crystals, respectively, because of their relatively large birefringence (typically >0.1).

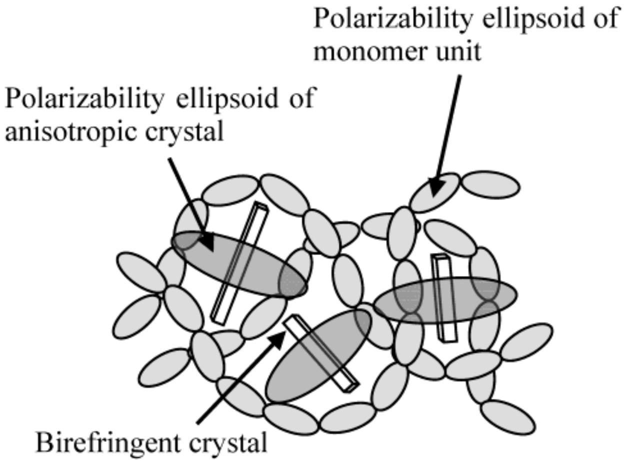

a) Random structure.

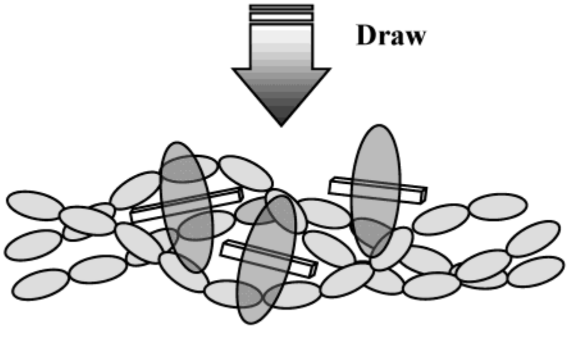

b) Orientation of a polymer and birefringent crystals by a heat drawing.

Figure 1. Mechanism of the compensation of orientational birefringence by the birefringent crystal dopant method.

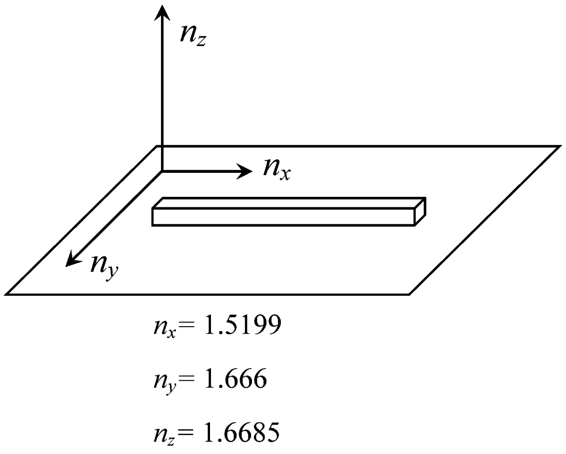

Figure 2. Structure and refractive indices of strontium carbonate crystal.

III. Experimental Section

Preparation of Strontium Carbonate ($SrCO_3$) Crystals and Polymer Film. $SrCO_3$ was selected in order to compensate the birefringence of polymers because the crystal is birefringent and needlelike. The structure of $SrCO_3$ crystal is illustrated in Figure 2. The refractive indices of $SrCO_3$ are $n_x = 1.5199$, $n_y = 1.666$, and $n_z = 1.6685$. $SrCO_3$ in a polymer is oriented with its long axis along its draw direction by tensile stress. Therefore, we defined the intrinsic birefringence Δn_c^0 of the $SrCO_3$ crystal as

$$\Delta n_c^0 = n_x - \sqrt{\frac{n_y^{\,2} + n_z^{\,2}}{2}} = -0.147 \tag{3}$$

The crystal has a negative orientational birefringence from this definition. $SrCO_3$ was prepared by a reaction of a suspension of strontium hydroxide with carbon dioxide. The surface of the crystal was modified by a titanate-based coupling agent [bis(dioctyl pyrophosphate) oxyacetate titanate] in order to disperse the crystal in the polymer homogeneously.

We selected methyl methacrylate (MMA) and benzyl methacrylate (BzMA) as monomers. A mixture of MMA, BzMA, and benzoyl peroxide as an initiator and *n*-butyl mercaptan as a chain transfer agent was placed in a glass tube. Polymerization was carried out at 70 °C for 1 day, yielding poly(MMA-*co*-BzMA) which had a positive birefringence, with the composition of MMA/BzMA = 78/22 (w/w). The bulk polymer obtained was heat-treated at 90 °C for 1 day in order to finalize the polymerization, and the bulk was dissolved in acetone. The polymer solution was filtered through a 0.2 μm membrane filter and dropped into methanol to precipitate the polymer and remove the remaining monomers. The polymer flakes obtained were dried under a reduced pressure for 2 days. Poly(MMA/BzMA = 78/22) was dissolved in tetrahydrofuran with the $SrCO_3$. The polymer solution was spread onto a glass plate using a knife coater to prepare film samples with a thickness of approximately 30 μm. Three types of film samples were prepared to evaluate the birefringent crystal dopant method. Film 1 was poly(MMA/BzMA=78/22), film 2 was 0.3 wt % of $SrCO_3$ doped polymer, and film 3 was 0.4 wt % of $SrCO_3$ doped polymer. These films were dried for 3 days at 90 °C at a reduced pressure (<1.33 Pa) to eliminate the solvent. The dried polymer films were uniaxially heat-drawn at a rate of 4 mm/min at 130 °C using a universal tensile testing machine (Tensilon RTC-1210A, A&D Co., Ltd.).

Sample Preparation for the Observation of $SrCO_3$ Crystals in Polymer Films. An epoxy resin (EPON-812), a curing agent, and an accelerating agent were mixed by stirring. After evacuation to remove any trapped air bubbles, the prepared film and the mixture were poured into blocks of capsular shape and hardened by keeping them for 24 h at 60 °C. The piece (300 μm × 300 μm × 300 μm) of the hardened epoxy polymer with the film was set in an ultracut microtome (FC-S, Reichert Jung) and was cut by a diamond knife to a thin slice with a thickness of 100 nm. The surface of the slice obtained was parallel to the draw direction. $SrCO_3$ in the slice was observed with a transmission electron microscope (TEM) (H-800, Hitachi, Ltd).

Measurements of the Birefringence of $SrCO_3$-Doped Polymer Film. The birefringence Δn of the drawn films was calculated by dividing the retardation of the films by the distance that the light propagated the films. The retardation was determined at a wavelength of 633 nm by optical heterodyne interferometry using birefringence measurement equipment (ABR-10A, Uniopt Corp., Ltd.).[19] The experimental setup is shown in Figure 3a. This system consists of a rotating half-wave plate, a rotating linear polarizer, a photodiode, an electric phase meter, and a frequency-stabilized transverse Zeeman laser (STZL) which has a two-frequency orthogonally polarized light source. The retardation and the principal axis direction of samples are measured by the analysis of the phase difference between the beat signal obtained and reference signal from the STZL. The relation between the incident direction of the light and the draw direction of the films is illustrated in Figure 3b, where θ_x and θ_y are the angles of incidence. The X axis is draw direction, and the Y axis is perpendicular to the X axis. The X and Y axes are in the film plane, and the Z axis is perpendicular to the film plane. Planes of incidence of the light are parallel to the $X-Z$ plane and the $Y-Z$ plane.

Measurements of Orientation Function of the Polymer Chain. To measure the degree of orientation of drawn polymer chains, the orientation function was determined from an infrared dichroic ratio measured by polarized Fourier transform infrared spectroscopy.[9,20] In a drawn polymer film, the polymer chains are preferentially oriented in the draw direction. The dichroic ratio D is defined by

$$D = A_{\parallel}/A_{\perp} \tag{4}$$

where $A_{\parallel}$ and $A_{\perp}$ are absorbances for linearly polarized infrared light in the parallel and perpendicular direction to the draw direction, respectively. $A_{\parallel}$ and $A_{\perp}$ of the drawn film were measured within the spectral range 400−4000 cm^{-1} using a Fourier transform infrared spectrometer (Digilab FTS-60A, Japan Bio-Rad Laboratories Co.). An orientation function f_D is related to the dichroic ratio D as

$$f_D = \frac{D-1}{D+2}\,\frac{2\cot^2\alpha + 2}{2\cot^2\alpha - 1} \tag{5}$$

where α is the angle between the transition moment vector of the absorbing group and the chain axis. We selected the symmetric bending of C-αCH_3 at 1388 cm^{-1} as the characteristic band of poly(MMA/BzMA=78/22). We used the angle α of 90° for the C-αCH_3 bending band that was determined by Zhao et al.[21]

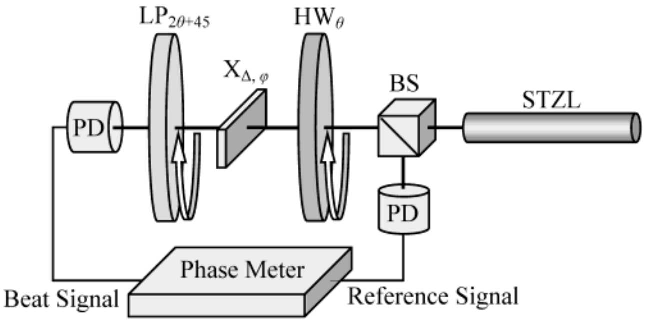

(a) Birefringence measurement equipment

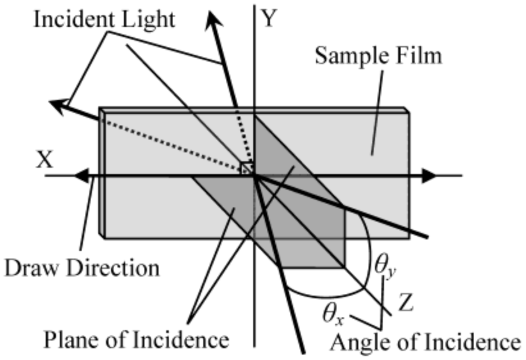

(b) Birefringence measured angle

Figure 3. Schematic diagram of a birefringence measurement by birefringence measurement equipment. (a) STZL is a stabilized transverse Zeeman laser, BS is a beam splitter, HW_θ is a half-wave plate that is set at a azimuthal angle θ, $X_{\Delta,\varphi}$ is a measurement sample with a phase difference Δ at a azimuthal angle φ, $LP_{\theta+45°}$ is a linear polarizer with a azimuthal angle θ + 45°, and PD is a photodiode. (b) A birefringence measurement of drawn films at an incident angle θ and φ of light.

Analysis of the Polarization Maintaining Property of the Polymer Films. The normalized light intensity at a wavelength of 633 nm through the center of the films between a polarizer and a rotating analyzer was measured to investigate the polarization maintaining property of the films. The experimental setup consists of a He−Ne laser, Glan-Taylor prisms as a polarizer and an analyzer, a power meter (Q8221, Advantest Corp.), and a digital lock-in amplifier (LI5640, NF Corp.) as shown in Figure 3. The films were placed between the polarizer and the analyzer, and the fast axis of the film was set at 45° to the transmitting direction of the polarizer. The normalized light intensity was measured as the analyzer was rotated every 0.2° from 0° (parallel polarizer state) to 90° (crossed polarizer state).

Other Measurements. The transmittance of undrawn films was measured using a spectrophotometer (U-2001, Hitachi instruments service Co., Ltd.). The haze of the films was measured according to American Society for Testing and Materials (ASTM) D1003. Furthermore, the T_g of the films was measured at a heating rate of 10 °C/min using a differential scanning calorimeter (DSC-50, Shimadzu Corp.).

IV. Results and Discussion

Observation of $SrCO_3$ Crystals Obtained and the Crystals in Polymer Films. The micrograph of synthesized crystals was taken using a scanning electron microscope (S-4700, Hitachi, Ltd.) as shown in Figure 5. The crystals had a needlelike shape with an average

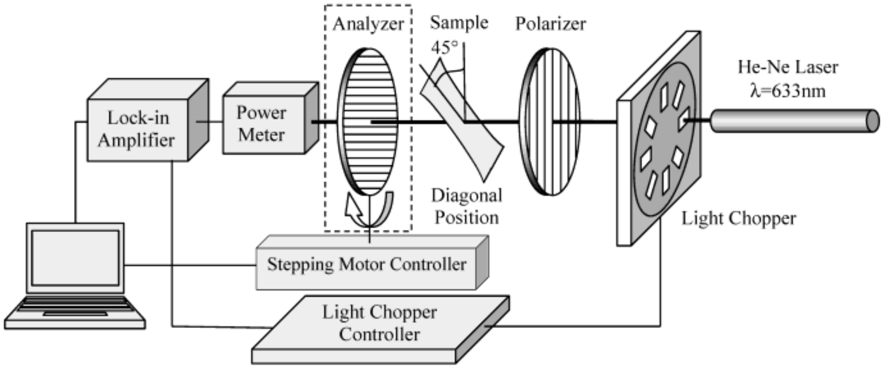

Figure 4. Experimental setup for the analysis of polarization maintaining property of $SrCO_3$-doped polymer films.

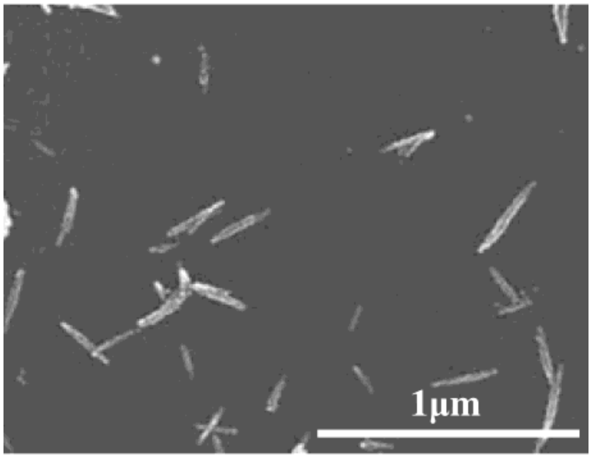

Figure 5. SEM micrograph of the synthesized $SrCO_3$ crystal.

length of about 200 nm and an average width of about 20 nm, from the observation of this micrograph.

Figure 6 shows TEM micrographs (×20000) of $SrCO_3$ doped into poly(MMA/BzMA=78/22) film at a concentration of 0.3 wt % and with a thickness of 100 nm (film 2). Dark images in the photographs are $SrCO_3$ crystals. The crystals were dispersed without aggregation because they were treated by a titanate-based coupling agent and were made hydrophobic. The crystals did not orient in the undrawn film as shown in Figure 6a. The orientation of the crystals to the draw direction of the film was observed after uniaxial heat drawing at a draw ratio about 2.0, as shown in Figure 6b. The crystals were oriented with the polymer orientation by external stress because they had a needlelike shape.

Birefringence Measurement of Drawn Polymer Films. The orientational birefringence Δn of the sample films was measured. The orientational birefringence Δn of the films against the draw ratio at an incident angle of 0° is shown in Figure 7. Undrawn films did not exhibit birefringence, and the birefringence of the heat-drawn films became larger in proportion to the draw ratio. Film 1 (poly(MMA/BzMA=78/22)) generated a positive birefringence because of the orientation of polymer chains. On the other hand, film 3, doped with 0.4 wt % of $SrCO_3$, exhibited a negative birefringence because of the orientation of the negative birefringent $SrCO_3$. In the case of film 2, the positive birefringence of the poly(MMA/BzMA=78/22) was compensated by doping with 0.3 wt % of $SrCO_3$ at any draw ratio. The birefringence of film 2 was less than 1.0×10^{-5}. These results confirmed that film 2 was a zero-birefringence optical polymer.

The orientational birefringence Δn of the drawn film 1 and film 2 against the incident angle of light was also measured, as shown in Figure 8. The draw ratio of the films was 2.0. Parts a and b of Figure 8 show the orientational birefringence of the drawn films that were measured at an incident angle θ_x in the $X-Z$ plane and at an incident angle θ_y in the $Y-Z$ plane, respectively. In Figure 8a, the sign of the birefringence was defined as positive when the refractive index in a parallel direction to the $X-Z$ plane was higher than that in a perpendicular direction. In Figure 8b, the sign of the birefringence was defined as positive when the refractive index in a parallel direction to X axis was higher than that in a perpendicular direction. The orientational birefringence of film 2 was compensated at the angle of

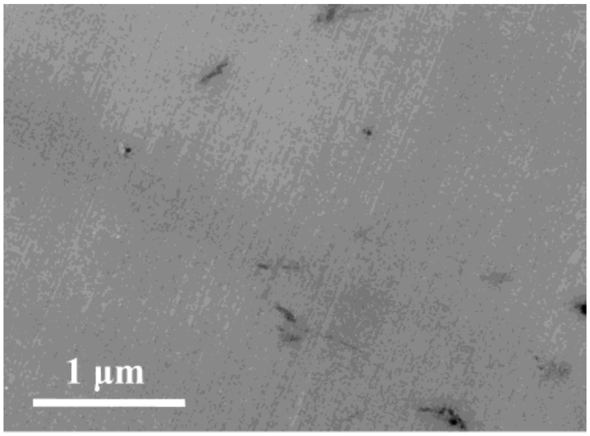

(a) Undrawn film.

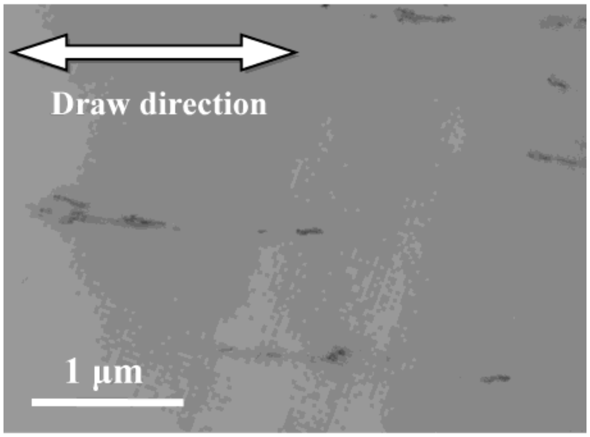

(b) Drawn film.

Figure 6. TEM micrographs of the $SrCO_3$ doped into poly(MMA/BzMA=78/22) film at a concentration of 0.3 wt % and with a thickness of 100 nm: (a) undrawn film; (b) drawn film at a draw ratio about 2.

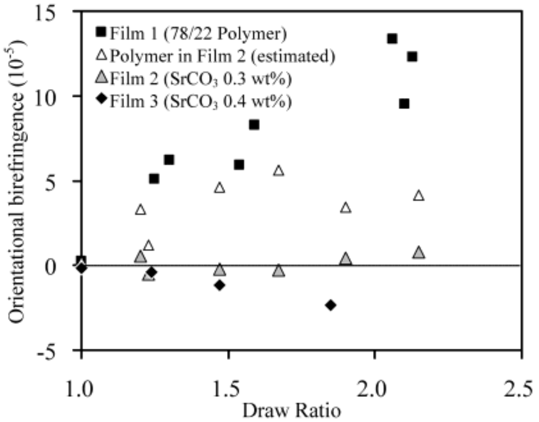

Figure 7. Orientational birefringence Δn of $SrCO_3$-doped poly(MMA/BzMA=78/22) film against a draw ratio, drawn at 130 °C and 4 mm/min.

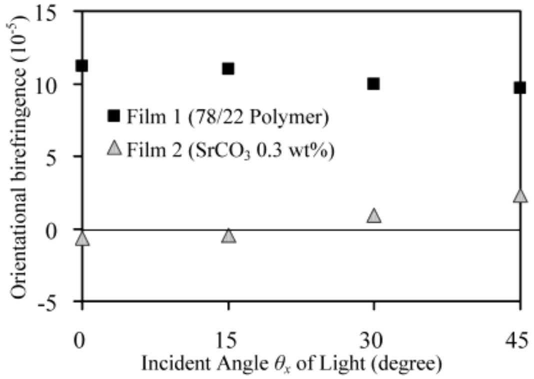

a) Orientational birefringence at an incident angle of θ_x.

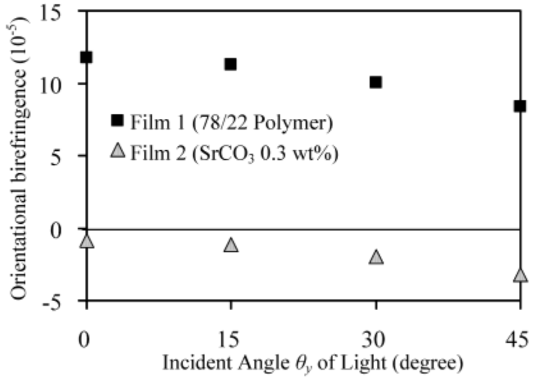

b) Orientational birefringence at an incident angle of θ_y.

Figure 8. Orientational birefringence Δn of $SrCO_3$-doped poly(MMA/BzMA=78/22) film, drawn at 130 °C and 4 mm/min and at a draw ratio of about 2: (a) orientational birefringence vs incident angle θ_x of light; (b) orientational birefringence vs incident angle θ_y of light.

0°. The birefringences of both film 1 and film 2 varied with the incident angle of light. The value of the negative birefringence of film 2 decreased, and the sign of the birefringence became positive when the angle θ_x of incidence of light became larger as shown in Figure 8a. The value of the negative birefringence of film 2 increased, when the angle θ_y became larger as shown in Figure 8b. From these results, we estimated that the refractive index n_z of drawn film 2 was higher than its n_x and n_y. The birefringences $\Delta n = n_z - n_y$ and $\Delta n = n_x - n_z$ were not zero, and very small birefringences still existed. However, the birefringence of film 2 was much lower than that of film 1 at any incident angle of light (0°−45°). These results indicated that the birefringence of film 2 depended on the incident angle, but the value of the birefringence of film 2 was much lower than that of film 1.

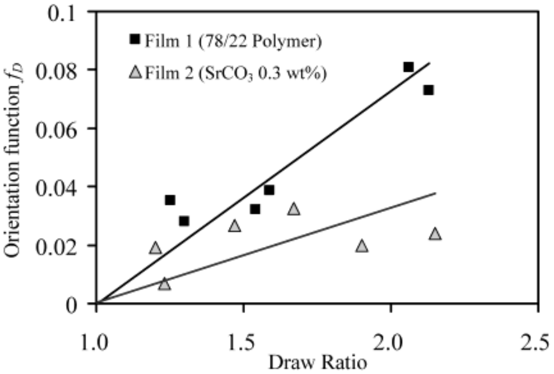

a) Orientation function f_D versus draw ratio.

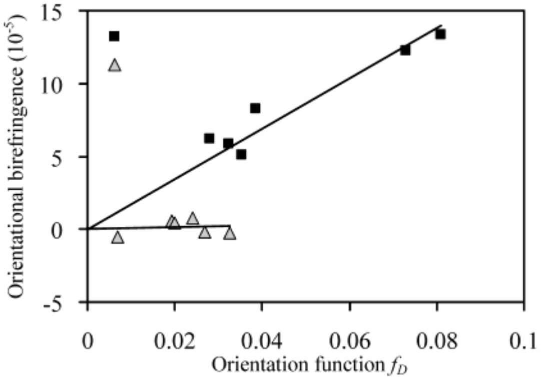

b) Orientational birefringence versus orientation function f_D.

Figure 9. Orientation function f_D of $SrCO_3$-doped poly(MMA/BzMA=78/22) film, drawn at 130 °C and 4 mm/min: (a) orientation function f_D vs draw ratio and (b) orientational birefringence vs orientation function f_D.

Orientation Functions of the Drawn Polymer Films. The orientation function f_D of the films was measured as shown in Figure 9. Square and triangular plots are measured data; straight lines are approximation curves. Figure 9a shows the orientation function against the draw ratio of the films, and Figure 9b shows the orientational birefringence of the films against the orientation function. The orientation function was calculated by eq 5. The orientation function of film 2 was about a half as large as that of film 1 at the same draw ratio as shown in Figure 9a. Figure 9b shows that film 2 had no birefringence at any orientation function of the poly(MMA/BzMA=78/22).

In Figure 9a, the slopes of the approximation curves of film 1 and film 2 were about 0.0729 and 0.0324, respectively. The orientation function of polymer chains was reduced by doping with $SrCO_3$ crystals. We have found the same reduction effect in the case of PMMA and PC doped with silica particles.[22] We called this effect “the orientation-inhibition effect”. The mechanism of the orientation-inhibition effect has not been clarified yet. The $SrCO_3$ crystals in film 2 inhibited the orientation of the polymer chain, and the generation of the birefringence of the polymer was reduced.

In the case of polymer blends, the orientational birefringence of the blends may be formulated by

$$\Delta n = \Delta n_1^0 f_1 \phi_1 + \Delta n_2^0 f_2 \phi_2 + \Delta n_{\mathrm{F}} \qquad (6)$$

where Δn_i^0 is the intrinsic birefringence of the *i* polymer, f_i is the orientation function, ϕ_i is the volume fraction, and Δn_F is the form birefringence.[9] We applied eq 6 to the following eq 7 in order to analyze the orientation phenomena of polymer molecules and $SrCO_3$ crystals in film 2.

$$\Delta n = \Delta n_p^0 f_p \phi_p + \Delta n_c^0 f_c \phi_c + \Delta n_F \qquad (7)$$

where subscripts p and c correspond to a polymer (poly(MMA/BzMA=78/22)) and a crystal ($SrCO_3$), respectively. The intrinsic birefringence of the polymer (Δn_p^0) was 0.00173 from the slope of the approximation curve in Figure 8b, and that of the crystal (Δn_c^0) was −0.147 from eq 3. The volume fraction of the polymer (ϕ_p) was 99.9055%, and that of the crystal (ϕ_c) was 0.0945%.

The birefringence caused by only the polymer molecules of film 2 was estimated as shown in Figure 7. The birefringence was the product of Δn_p^0, ϕ_p, and the orientation function of the polymer main chains of film 2 shown in Figure 9 as f_p. The difference between the estimated birefringence and the measured birefringence of film 1 was the birefringence reduction by the orientation-inhibition effect. Furthermore, difference between the estimated birefringence and the measured birefringence of film 2 was the birefringence reduction by the negative birefringence of the $SrCO_3$ crystals.

The orientation function of $SrCO_3$ was calculated by the following eq 8

$$f_c = (\Delta n - \Delta n_p^0 f_p \phi_p - \Delta n_F)/(\Delta n_c^0 \phi_c) \qquad (8)$$

which leads from eq 7. The birefringence of film 2 shown in Figure 7 was used for Δn, and the orientation function of the polymer shown in Figure 9 was used for f_p. The above-mentioned values were used for Δn_p^0, Δn_c^0, ϕ_p, and ϕ_c. In our case, it is difficult to calculate the form birefringence Δn_F because $SrCO_3$ crystal is an optically anisotropic material, and the orientation function of the crystal is not 1. We assumed the orientation function to be 1 (completely oriented state) and the refractive index of $SrCO_3$ to be the average refractive index of $SrCO_3$. The estimated Δn_F was low ($<1.0 \times 10^{-5}$) and positive and did not compensate the positive birefringence of the polymer; therefore, Δn_F was assumed to be zero following eq 9

$$\Delta n_F \cong 0 \qquad (9)$$

f_c was calculated by substituting the values described above into eq 8. The calculation of f_c against the orientation function of the polymer is shown in Figure 10. In this figure, the slope of the approximation curve was about 12.0. We found out the calculated orientation function of the crystal was about 12.0 times larger than that of the polymer in the drawing condition. These results showed that the birefringence of the film was compensated by a low concentration of $SrCO_3$ because of its orientation-inhibition effect and its high orientation degree as compared with that of the polymer main chains.

Polarization Maintaining Property. Figure 11 shows the polarization-maintaining property of the undrawn films (Figure 11a) and the heat-drawn films (Figure 11b) of film 1 and film 2 at a draw ratio about 2.2 and from the rotating angles of 88°−90°. The data for air were measured without the films in place. The data for air represent the detection limit of our experimental setup. These data were normalized by light intensities at 0° (parallel polarizers state). The undrawn films had no birefringence as shown in Figure 7. Therefore, the normalized light intensity of the films was the same as the intensity at the detection limit, as shown in Figure 11a. This measurement confirmed that the crystal in film 2 did not disturb the polarization state of incident light, and film 2 was a uniform material because the crystal was smaller than the wavelength of the light. Figure 11b shows that the normalized light intensity of air was 0.303×10^{-4} in the crossed polarizers state (90°). This value is the extinction ratio of our experimental setup. The extinction ratio of drawn film 1 was 2.069×10^{-4} because of the birefringence caused by the heat-drawing. On the other hand, the extinction

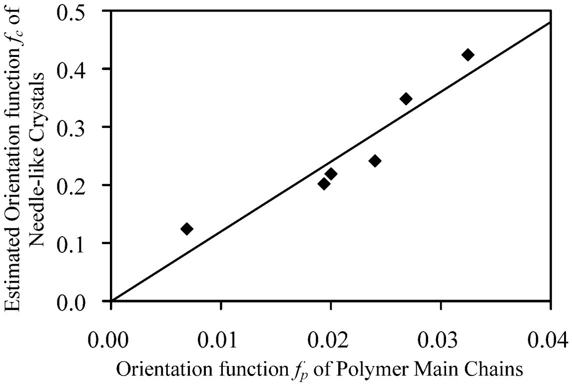

Figure 10. Estimated orientation function f_c of $SrCO_3$ needle-like crystals in the crystal-doped poly(MMA/BzMA=78/22) films (film 2) against the orientation function f_p of a polymer main chain of the films.

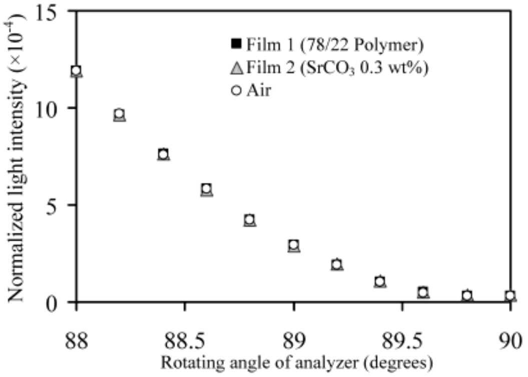

a) Undrawn films.

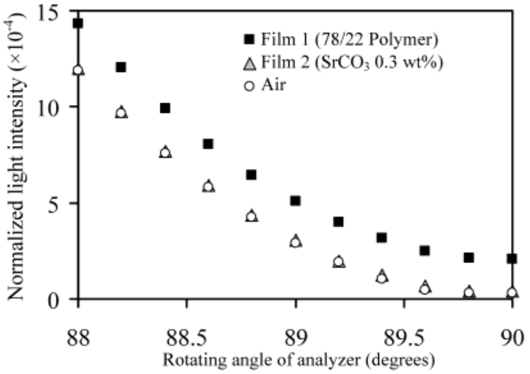

b) Drawn films.

Figure 11. Normalized light intensity of $SrCO_3$-doped poly(MMA/BzMA=78/22) films at a draw ratio of 2.15 between a polarizer and an analyzer: (a) undrawn films and (b) drawn films at a draw ratio about 2.2.

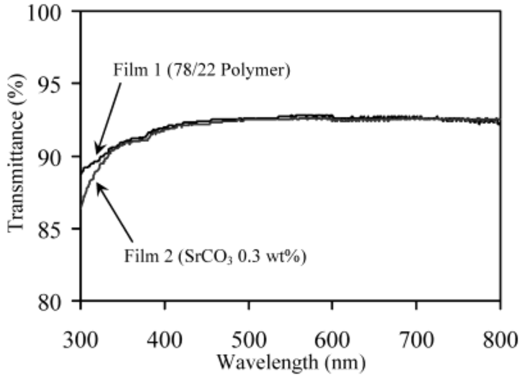

Figure 12. Transmittance of $SrCO_3$-doped poly(MMA/BzMA=78/22) films.

Table 1. Haze and T_g of $SrCO_3$-Doped Poly(MMA/BzMA=78/22) Films

	haze (%)	T_g (°C)
film 1	0.5	109.4
film 2	0.6	109.6

ratio of drawn film 2 was 0.396×10^{-4}. Film 2 maintained the polarization state of incident light almost at the detection limit because it had no birefringence. From these results, we confirmed that the polarization-maintaining property was considerably improved by compensating the birefringence of the films.

Transparency and Thermostability. The transmittances of film 1 and film 2 were measured as shown in Figure 11. The transmittances of film 1 and film 2 at a wavelength of 633 nm, at which the birefringence was measured, were 92.6% and 92.5%, respectively. The transmittance of film 2 was maintained in as broad a wavelength region as film 1. The transmittance below a wavelength of about 350 nm was reduced because the length of $SrCO_3$ crystals in film 2 was close to the wavelength. The haze and the T_g of film 1 and film 2 are shown in Table 1. Doping with $SrCO_3$ increases the haze and T_g by 0.1% and 0.2 °C, respectively. However, they were almost the same as those of the undoped film (film 1). It should be noted that $SrCO_3$ compensated the positive birefringence of the polymer while maintaining the transparency and thermostability of the undoped films.

V. Conclusions

We have demonstrated the birefringent crystal dopant method by homogeneous doping with $SrCO_3$ to compensate for the orientational birefringence of a polymer. $SrCO_3$ in the drawn polymer film was oriented to the draw direction with the polymer main chain from TEM observations. As a result, the positive birefringence of heat-drawn poly(MMA/BzMA=78/22) films at a wavelength of 633 nm was compensated by doping with 0.3 wt % of $SrCO_3$ while maintaining film transparency and thermostability. At any incident angle of light, the birefringence of the $SrCO_3$-doped polymer films was much lower than that of the undoped films. The analysis of the orientation function of the films showed that the birefringence of the films was compensated at a low concentration of $SrCO_3$ because of its orientation-inhibition effect and its high orientation degree as compared with those of the polymer chains. Furthermore, we confirmed that the zero-birefringence film almost maintained the polarization state of the incident light.

References and Notes

(1) Ishigure, T.; Nihei, E.; Koike, Y. *Appl. Opt.* **1994**, *33*, 4261.
(2) Koike, Y.; Ishigure, T.; Nihei, E. *J. Lightwave Technol.* **1995**, *13*, 1475.
(3) Mori, H.; Itoh, Y.; Nishiura, Y.; Nakamura, T.; Shinagawa, Y. *Jpn. J. Appl. Phys.* **1997**, *36*, 143.
(4) Bernacki, E.; Mansuripur, M. *Appl. Opt.* **1993**, *32*, 6547.
(5) Koike, Y.; Tanio, N.; Nihei, E.; Ohtsuka, Y. *Polym. Eng. Sci.* **1989**, *29*, 1200.
(6) Koike, Y.; Takezawa, Y.; Ohtsuka, Y. *Appl. Opt.* **1988**, *27*, 486.
(7) Hecht, E. *Optics*, 4th ed.; Addison-Wesley: New York, 2002.
(8) Born, M.; Wolf, E. *Principles of Optics*, 7th (expanded) ed.; Cambridge University Press: New York, 1999.
(9) Saito, H.; Inoue, T. *J. Polym. Sci., Part B* **1987**, *25*, 1629.
(10) Bragg, W. L.; Pippard, A. B. *Acta Crystallogr.* **1953**, *6*, 865.
(11) Van Krevelen, D. W. *Properties of Polymers*, 3rd ed.; Elsevier: Dordrecht, 1990.
(12) Meeten, G. H. *Optical Properties of Polymers*; Elsevier Applied Science Publishers: Dordrecht, 1986.
(13) Hahn, B. R.; Wendorff, J. H. *Polymer* **1985**, *26*, 1619.
(14) Iwata, S.; Tsukahara, H.; Nihei, E.; Koike, Y. *Jpn. J. Appl. Phys.* **1996**, *35*, 3896.
(15) Iwata, S.; Tsukahara, H.; Nihei, E.; Koike, Y. *Appl. Opt.* **1997**, *36*, 4549.
(16) Tagaya, A.; Iwata, S.; Kawanami, E.; Tsukahara, H.; Koike, Y. *Appl. Opt.* **2001**, *40*, 3677.
(17) Tagaya, A.; Iwata, S.; Kawanami, E.; Tsukahara, H.; Koike, Y. *Jpn. J. Appl. Phys.* **2001**, *40*, 6117.
(18) Tagaya, A.; Ohkita, H.; Mukoh, M.; Sakaguchi, R.; Koike, Y. *Science* **2003**, *301*, 812.
(19) Umeda, N.; Kohwa, H. *Electron. Commun. Jpn., Part 2* **1991**, *74*, 21.
(20) Jasse, B.; Koenig, J. L. *J. Macromol. Sci., Rev. Macromol. Chem.* **1979**, *C17*, 61.
(21) Zhao, Y.; Jasse, B.; Moneie, L. *Makromol. Chem., Macromol. Symp.* **1986**, *5*, 87.
(22) Ohkita, H.; Abe, Y.; Kojima, H.; Tagaya, A.; Koike, Y. *Appl. Phys. Lett.* **2004**, *84*, 3534.

MA049296+